# IDENTIFYING CORTICAL SULCI FROM LOCALIZATION, SHAPE AND LOCAL ORGANIZATION

*Matthieu Perrot[123], Denis Rivière[13], Jean-François Mangin[123]*

[1]Neurospin, CEA, Saclay, France
[2]INSERM U.797, Orsay, France
[3]IFR 49, Paris, France

## ABSTRACT

In this paper we propose an approach to identify sulci from sulcal pieces. Our method is founded on the sulci localization, feature-based shapes and their local organization. The position data enable the devising of an easy handled 3D probabilistic atlas using SPAM models. Shapes and local sulci scheme are recognized thanks to SVR models (a regression version of Support Vector Machine). All these aformentioned aspects are merged into a unified markovian framework, which favours locally the most reliable information. The first model is used to strongly constrain label coverage over space and the second to reach coherence within sulci neighbourhood. The mixture outperforms both models taking the best of their local performances.

***Index Terms—*** cortical folds labeling, sulci, SPAM, SVR, Hidden Markov Field

## 1. INTRODUCTION

Brain cortex surface draws complex folds patterns known as sulci, related to a mixture of genetic and developmental rationales, mechanical and connectivity constraints. Moreover, we do not really know the extent of the connections between cortical areas defined by sulci and functional activity. Especially, understanding the folding process can help to reduce inter-individual variability in functional studies, or study the links between abnormal brain developpement and psychiatric pathologies. Some preliminary studies on cortex asymmetry and sex retrieval [1] use a recognition system from our previous works [2].

Anatomists attempt to find steady patterns among sulci variability. It leads to some consensus about large structures which can be divided in primary, secondary and tertiary sulci according to their appearance order during brain development. Then, the earlier a sulcus appears, the lower is the variability within population. In this study, we consider sulci labels based on the sulcal roots theory [3] founded on Régis works, but other nomenclatures exist for unsteady structures. This theory predicts that several patterns could coexist within the same class according to sulcal roots prefered orientation leading to broken or connected sulcus [4]. This emphasizes the complexity of defining a shape model.

Some authors focus on shape-based recognition through the definition of sketched sulci : sulcal lines [5] [6] neglecting branches or breaks, sulcal ribbons [7] without branches but with breaks, sulcal pieces [2] [8] [9], surfaced sulcal pieces [10]. Others concentrate on localized features along the cortex surface [11] [10] [12] or over MRI voxel space [13]. Sometimes interaction between sulci are considered through markovian assumptions [2] [11]. Position or shape information is sufficient to recognize primary sulci (most authors consider often about 10 sulci [10] [13] [5] [7]), but both information is required for secondary or tertiary sulci (studied by [11] [12] [2] through 40 to 60 sulci). Thus, in the following, we propose a refinement of our previous recognition system with the addition of a model of the localization of sulci. This Bayesian model is quite close to the ones in [8] [7] but combined into the markovian framework of our previous works.

## 2. METHODS

Labeling of sulci consists in assigning one label $l_i$ to each sulcal elementary piece $L_i$ (most of the time we confuse $l_i$ and $L_i$ to lighten notations). Inference of a labeling $L$ from data $D$ and priors can be understood into this general Bayesian formulation :

$$P(\mathbf{Labeling}|\mathbf{Data}) = P(L|D) \propto P(D|L)P(L)$$

Two related standard Bayesian risks can express the worth of errors :

- MAP (Maximum a posteriori) : each erroneous global labeling has the same cost.

$$L^*_{\text{MAP}} = \arg\max_L P(L|D)$$

- MPM (Marginal Posterior Mode [14]) : each local error has the same cost. It adds a gradient to the preceding Bayesian risk.

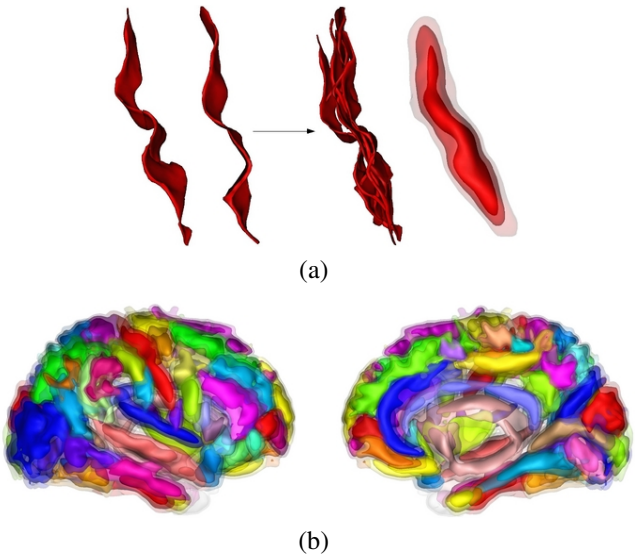

(a)

(b)

**Fig. 1**. (a) : SPAM results from counting sulci over voxels, filtering it with gaussian blur and normalizing the result to yield a 3D probability map. Above, we display several central sulci and the resulting SPAM. (b) lateral and medial views of SPAM of 60 coloured sulci. (a-b) : SPAM are represented here by 3 surfaces with various levels of transparency based on a thresholding of the probability map preserving 30, 60 and 80 percent of the distribution core.

$$L^*_{\text{MPM}} = \{L^*_i\}_{i\in\mathcal{L}} = \left\{ \arg\max_{L_i} P(L_i|D) \right\}_{i\in\mathcal{L}}$$

with $L_i$ the labeling of one sulcus piece and $\mathcal{L}$ the set of all sulcus pieces.

Without any additional hypothesis, MAP can be optimized by simulated annealing coupled with Gibbs sampling to approach global energy minimum or by ICM (Iterated Conditional Mode) to only reach the nearest local energy minimum. MPM criterion is assessed by a Markov Chain Monte Carlo (MCMC) method which boils down to a Gibbs sampling over labels on each sulcal piece of which the most frequent label is taken.

In this context, we present three models : the first one is based only on localization information, the second one on shapes and organization of sulci, the last one is a combination of both.

### 2.1. Localization model : SPAM

Sulci are rather well localized so we try to take advantage of this assumption through SPAM (Statistical Probabilistic Anatomy Map [15]) models which provides voxelwise probabilities. To see SPAM in the context of modeling sulci, the reader is referred to [8]. Here, $D=\{D_i\}_{i\in\mathcal{L}}$ represents localizations of each sulcus piece $L_i$ (see figure 1).

Under conditional independency assumptions between local sulci model we can derive a naive Bayesian classifier (MPM and MAP are equivalent here):

$$L^*_{\text{SPAM}} = \{L^*_i\}_{i\in\mathcal{L}} = \left\{ \arg\max_{L_i} \frac{P(D_i|L_i=l_i)\ P(L_i=l_i)}{\sum_{l_j} P(D_i|L_i=l_j)\ P(L_i=l_j)} \right\}_{i\in\mathcal{L}}$$

with $\{l_i\}$ is the set of enabled labels for each sulcal piece.

Above, the normalization term (the denominator) is tractable so posterior probabilities can be obtained. Each sulcal piece likelihood $P(D_i|L_i)$ is computed according to statistical independence assumptions between each of its voxels. Finally mean log-likelihood is rather used to erase the influence of voxels number. $P(L)$ is our prior on labeling. For this localization model and the full one, we take a simple measure of labels frequencies over sulcal pieces.

### 2.2. Shapes and local organization of sulci : SVR

In our previous works [2], we introduced a sulci recognition system based on high level percepts : features describing morphological and topological properties of cortical folds. Based on dedicated local experts, each sulcus shape is learned apart from others and local sulci arrangement is learned from pairs of sulci. These models are embeded as clique potentials in a global markovian framework where we supposed only local interactions was governing sulcal organization. MAP or MPM probability inferences under markovian dependencies rather focus on the associated Gibbs energy $E(L)$ because only local energy differences between involved states are needed. It is expressed over clique potentials $\psi_c$ based on sulci and pairs of sulci as below :

$$P(L|D) = \frac{P(D,L)}{P(D)} = \frac{e^{-E(L)}}{P(D)}$$

$$E(L) = -log\Big(P(D,L)\Big) = -log\Big(\prod_{c\in\mathcal{C}} P(D_c L_c)\Big) = \sum_{c\in\mathcal{C}} \psi_c(D_c,L_c)$$

with $P(D)$ the normalization constant which is independent of the labeling.

In this paper, we substitute our former potential models (Multi Layer Perceptrons) for SVR (Support Vector Regression) in order to avoid fastidious definition of neural network topology, black box approach that prevents good interpretability. Finally, it improves versatility which allows easy future additions or redefinings of data features. Furthermore, large band model like SVR are more constrained and better suited in large dimension problems.

### 2.3. Mixture : SPAM + SVR

Several approaches can be expressed to mix the two preceding models and study the influence of spatial information. The simplest and fastest one is to use the SPAM model to initialize a labeling and fall into the first local minimum of the optimized MAP criterion with ICM.

Results show that many local SPAM posterior probabilities of labels are almost zero. In our previous works we locally limit the size of the state space (the set of enabled labeling) thanks to a coarse modelisation of each sulcus localization (each label is restrained within a bounding box [2]). SPAM are more accurate and restrictive, so we can use them to spatially constrain labels presence. Only labels with a posterior probability over a really low threshold (0.01 in our experiments) are preserved. The same can be derived for MPM or MAP with Gibbs sampling at low temperature. These approaches assume that the initialization is really good, close to the optimal answer and only slight local changes are still needed.

Under sensible independence assumptions between each kind of information (localization, shape, local organization), we rewrite $D=\{D_p\}\{D_s\}\{D_{st}\}$ over sulcal pieces, sulci and sulcal pairs. Thus, a better sharp coupling integrates each model into one probability (MAP below).

$$P(D|L) = \prod_{i \in \underset{\text{pieces}}{\text{sulcal}}} P(D_i|L_i) \prod_{s \in \text{sulci}} P(D_s|L_s) \prod_{s\,t \in \underset{\text{pairs}}{\text{sulcal}}} P(D_{st}|L_{st})$$

where $L_i$ is the label of sulcal piece $i$, $L_s$ is the set of sulcal pieces of sulcus $s$, $L_{st}$ is the set of sulcal pieces of sulci $s$ and $t$.

We know that none of the models is reliable or steady enough. In fact some sulci are really well localized, others have a well defined shape. This kind of information should be balanced to favour those which can be believed. We suggest that each likelihood $P(D_i|L_i)$ is flattened in accordance with error rates $e_i$ measured on an unused learning database.

## 3. RESULTS AND DISCUSSION

We used in our experiments the same database (identical labeling and segmentation) as in [2]. It is composed of 26 manually labeled Right brains from healthy subjects : 21 are used to train our system (16 to learn local models and 5 to rate each model to enhance reliable models influence in the global optimized energy) and 5 to evaluate its generalization ability. All brains are transformed using rigid registration into the Talairach coordinates system and scaled to reduce global size variability.

SPAM-based model 2.1 is really fast to learn and gives better recognition rates than our previous model on healthy subjects. But for human experts some errors are intolerable, so their assessment may not match recognition rates. So, serious errors (huge sulci parts missing, double outlines) happen even on quite stable sulci (central sulcus for instance when localization is ambiguous or deviant from the learned model) and furthermore we notice a great sensitivity to segmentation errors.

Thus high level information remains required, even though error rates of our SVR-based model 2.2 are higher.

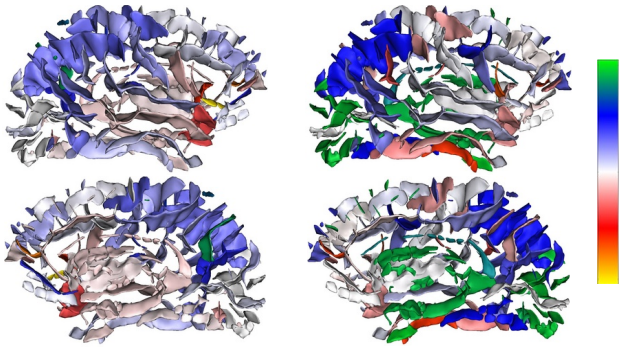

(a) localization model (b) shape and organization model

**Fig. 2**. Color mapping of average sulcuswise error differences of single models (localization model SPAM (a) and shape+organization model SVR (b)) versus full model (SPAM + SVR) on an arbitrary subject. Values range from $-21\%$ (yellow) to $+21\%$ (green) with white color for null value. Green and blue values show an improvement of the mixture model against the single ones, read and yellow for the opposite.

Indeed, its labeling generates more consistent sulcal shapes and patterns, that is the reason why both models are valuable. Several combinations are of interest (see 2.3) and all give promising results (see table 1). Improvements supplied by our best model are highlighted in figure 2 with respect to the SPAM model 2.1.

Sulcuswise error rates (figure 2) penalize each wrong-labeled sulcal piece, involving the considered sulcus, in relation to its size (see [2]). Each extra or missing sulcal piece is considered, thus the displacement of a sulcus is taken into account twice. Two global errors have been derived from local ones. For 'mass error', size weights are relative to the sum of all sizes (large sulci have more importance), whereas for 'mean error', size weights are only normalized by the sum of local sulcal pieces involved in its computing (each sulcus has the same weight but small sulcal pieces are less influent than greater ones). The second error rates help thus to focus on small sulci and highlights some enhancements (see Table 1).

## 4. CONCLUSION AND PERSPECTIVES

Brain anatomy outlines complex patterns that we can not claim to learn only by localized information. However, atlas-based approaches offer some coarse insights that we can not afford to omit. These local models are often elementary and offer easy ways to represent, compare and explain data. Indeed, SPAM priors give some useful information about localization and shape tendencies. So, it helps to refine spatial labels restriction in the limit of sulci localization variability, but allow ever some local adjustements to take into account

| | | Single Models | | Models Mixture | | |
|---|---|---|---|---|---|---|
| | | SPAM | SVR + Gibbs | SPAM init SVR + ICM | SPAM init SVR + MPM | SPAM potential SVR + Gibbs |
| mass error | train | 10.33 | 19.81 | 11.39 | 14.18 | 9.90 |
| | test | 21.42 | 26.70 | 21.76 | 20.46 | 19.14 |
| mean error | train | 21.82 | 32.12 | 22.09 | 27.11 | 19.17 |
| | test | 43.08 | 44.72 | 41.71 | 39.46 | 38.04 |

**Table 1**. Error rates on train and test databases for several models. From left to right, separated models : SPAM only (2.1), SVR only (2.2), models mixture. "SPAM init" means : initialization and pruning based on SPAM model. "SPAM potential" means a full coupling through the markov field between both isolated models. "SVR + *mode*" : here *mode* specifies the optimization method used for labeling.

the shape of sulci. With such addition to our previous works, we reduce combinatory of sulcus pieces a lot, ensure a reduction of the number of local minima, enhance recognition rates and speed-up the computing. So, we demonstrate that a combination of localization, shape and local organization models is able to manage well cortical folds.

Now, deepest analyses of errors are needed in regard to additional data so as to understand which information is currently missing in the model or underexploited (sulcal roots, steady sulci organization patterns...). Especially, we already consider alternative shape models to provide better description of sulci based on SPAM definition from local coordinate systems. In addition, extracting relevant information from the existing recognition system is worthwhile to make the models simpler and locally focus on features of matter. We now intend to evolve our recognition system incorporating functional (position of activation) or diffusion (white fibers) data to improve our comprehension of brain organisation through their existing links, each modality providing clues to better understand the others.

## 5. REFERENCES


[1] E. Duchesnay, A. Cachia, A. Roche, D. Rivière, Y. Cointepas, D. Papadopoulos-Orfanos, M. Zilbovicius, J. Martinot, J. Régis, and J. Mangin, "Classification based on cortical folding patterns.," *IEEE Trans Med Imaging*, vol. 26, no. 4, pp. 553–65, 2007.

[2] D. Rivière, J.-F. Mangin, D. Papadopoulos-Orfanos, J.-M. Martinez, V. Frouin, and J. Régis, "Automatic recognition of cortical sulci of the human brain using a congregation of neural networks," *Medical Image Analysis*, vol. 6, no. 2, pp. 77–92, 2002.

[3] J. Régis, J.-F. Mangin, T. Ochiai, V. Frouin, D. Rivière, A. Cachia, M. Tamura, and Y. Samson, ""sulcal root" generic model: a hypothesis to overcome the variability of the human cortex folding patterns," *Neurol Med Chir (Tokyo)*, vol. 45, pp. 1–17, 2005.

[4] Z. Y. Sun, D. Rivière, F. Poupon, J. Régis, and J.-F. Mangin, "Automatic inference of sulcus patterns using 3d moment invariants," *MICCAI*, 2007.

[5] S. Kobashi, S. Sueyoshi, K. Kondo, and Y. Hata, "Automated gyrus labeling using knowledge-based fuzzy inference systems," *System of Systems Engineering, 2007. SoSE '07. IEEE International Conference on*, pp. 1–6, 16-18 April 2007.

[6] X. Tao, J. L. Prince, and C. Davatzikos, "Using a statistical shape model to extract sulcal curves on the outer cortex of the human brain," *IEEE Trans. Med. Imaging*, vol. 21, no. 5, pp. 513–524, 2002.

[7] I. Corouge, *Modélisation statistique de formes en imagerie cerebrale*, Ph.D. thesis, Université de Rennes I, mention informatique, April 2003.

[8] G. Le Goualher, D. L. Collins, C. Barillot, and A. C. Evans, "Automatic identification of cortical sulci using a 3d probabilistic atlas," in *MICCAI '98: Proceedings of the First International Conference on Medical Image Computing and Computer-Assisted Intervention*, 1998, vol. 1496, pp. 509–518.

[9] A. Klein and J. Hirsch, "Mindboggle: a scatterbrained approach to automate brain labeling.," *Neuroimage*, vol. 24, no. 2, pp. 261–280, January 2005.

[10] K. J. Behnke, M. E. Rettmann, D. L. Pham, S. M. Resnick D. Shen, C. Davatzikos, and J. L. Prince, "Automatic classification of sulcal regions of the human brain cortex using pattern recognition," *Proceedings of SPIE Medical Imaging 2003: Image Processing*, vol. 5032, pp. 1499–1510, 2003.

[11] B. Fischl, A. van der Kouwe, C. Destrieux, E. Halgren, F. Ségonne, D. H. Salat, E. Busa, L. J. Seidman, J. Goldstein, D. Kennedy, V. Caviness, N. Makris, B. Rosen, and A. M. Dale, "Automatically parcellating the human cerebral cortex.," *Cereb Cortex*, vol. 14, no. 1, pp. 11–22, January 2004.

[12] G. Lohmann and D. Y. von Cramon., "Automatic labelling of the human cortical surface using sulcal basins," *Medical Image Analysis*, vol. 4, no. 3, pp. 179–188, 2000.

[13] Z. Tu, S. Zheng, A.L. Yuille, A.L. Reiss, R.A. Dutton, A.D. Lee, A.M. Galaburda, I. Dinov, P.M. Thompson, and A.W. Toga, "Automated extraction of the cortical sulci based on a supervised learning approach.," *IEEE Trans Med Imaging*, vol. 26, no. 4, pp. 541–52, 2007.

[14] M. Comer and E. Delp, "Multiresolution image segmentation," *Proc. 1995 IEEE Int. Conf. Acoustics, Speech, and Signal Processing*, pp. 2415–2418, 1995.

[15] A.C. Evans and et al., *Three-Dimensional Correlative Imaging: Applications in Human Brain Mapping*, chapter 14, pp. 145–161, Functional Neuroimaging, 1994.